

· 临床研究 ·

## 基于B超特征构建外侧象限乳腺癌腋窝淋巴结转移列线图预测模型

朱美娣<sup>1</sup>, 许紫鹏<sup>2</sup>, 华玲玲<sup>1</sup>, 秦菲<sup>3</sup>, 房灵<sup>4</sup>, 陈超波<sup>2\*</sup>

<sup>1</sup>无锡市锡山人民医院超声科, <sup>2</sup>普外科, 江苏 无锡 214105; <sup>3</sup>江南大学附属无锡五院(无锡市第五人民医院)超声科, 江苏 无锡 214011; <sup>4</sup>无锡市锡山人民医院皮肤科, 江苏 无锡 214105

**[摘要]** 目的: 回顾性分析外侧象限乳腺癌患者乳腺原发肿瘤及腋窝淋巴结的超声特征, 并构建列线图模型, 为临床评估外侧象限乳腺癌患者腋窝淋巴结转移提供影像学依据。方法: 回顾性分析无锡市锡山人民医院经病理证实的127例外侧象限乳腺癌患者腋窝淋巴结及乳腺原发肿瘤的超声影像学特征。伴腋窝淋巴结转移者分入阳性组(54例), 不伴腋窝淋巴结转移者分入阴性组(73例)。采用单变量和多变量Logistic回归分析, 筛选淋巴结转移的危险因素。使用R语言将数据集随机分成训练集和验证集, 基于训练集构建列线图预测模型, 预测腋窝淋巴结转移风险, 并在验证集中验证。受试者工作特征(receiver operating characteristic, ROC)曲线用于评估诊断性能, 校正曲线和Hosmer-Lemeshow检验用于评估预测值与实际列线图预测值的一致性。结果: 肿瘤针状边缘(OR=4.16, 95%CI: 1.25~13.79)和淋巴门结构不清晰(OR=19.20, 95%CI: 1.98~186.36)是外侧象限乳腺癌患者发生腋窝淋巴结转移的独立危险因素。据此构建预测外侧象限乳腺癌腋窝淋巴结转移的列线图模型。ROC曲线显示, 训练集的曲线下面积(area under curve, AUC)为0.74(0.62~0.86), 验证集AUC为0.73(0.62~0.84)。训练集和验证集的Hosmer-Lemeshow检验分别为 $P=0.570$ 和 $P=0.552$ 。结论: 超声有助于术前外侧象限乳腺癌患者腋窝淋巴结转移情况的评估; 基于Logistic回归构建的列线图预测模型具有良好的安全性、可靠性和实用性。

**[关键词]** 超声; 外侧象限乳腺癌; 腋窝淋巴结转移; 列线图; Logistic回归

**[中图分类号]** R445.1

**[文献标志码]** A

**[文章编号]** 1007-4368(2025)01-13-09

**doi:** 10.7655/NYDXBNSN240711

## Development a nomogram predictive model for axillary lymph node metastasis in lateral quadrant breast cancer based on B-ultrasound features

ZHU Meidi<sup>1</sup>, XU Zipeng<sup>2</sup>, HUA Lingling<sup>1</sup>, QIN Fei<sup>3</sup>, FANG Ling<sup>4</sup>, CHEN Chaobo<sup>2\*</sup>

<sup>1</sup>Department of Ultrasound, <sup>2</sup>Department of General Surgery, Xishan People's Hospital of Wuxi City, Wuxi 214105;

<sup>3</sup>Department of Ultrasound, Affiliated Wuxi Fifth Hospital of Jiangnan University (the Fifth People's Hospital of Wuxi), Wuxi 214011; <sup>4</sup>Department of Dermatology, Xishan People's Hospital of Wuxi City, Wuxi 214105, China

**[Abstract]** **Objective:** To retrospectively analyze the ultrasound features of primary breast tumors and axillary lymph nodes in patients with lateral quadrant breast cancer, and to construct a nomogram model to provide imaging evidence for better clinical assessment of axillary lymph node metastasis in these patients. **Methods:** We retrospectively analyzed ultrasonographic features of the axillary lymph nodes and primary breast tumors in 127 patients with lateral quadrant breast cancer, confirmed by pathology at Xishan People's Hospital of Wuxi City. Patients with axillary lymph node metastasis were categorized into the positive group (54 cases), while those without axillary lymph node metastasis were classified into the negative group (73 cases). Univariate and multivariate logistic regression analyses were performed to identify the risk factors for lymph node metastasis. The dataset was randomly divided into a training set and a validation set using the R language. A nomogram prediction model was constructed based on the training set to predict the risk of axillary lymph node metastasis and validated in the validation set. Diagnostic performance was evaluated using receiver operating characteristic (ROC) curves, while calibration curves and the Hosmer-Lemeshow test were used to assess the consistency between the predicted and actual values of the nomogram. **Results:** Tumor spiculated margin (OR=4.16, 95% CI:

**[基金项目]** 国家自然科学基金(82302562); 无锡市卫健委后备拔尖人才项目(HB2023116)

\*通信作者(Corresponding author), E-mail: bobo19820106@gmail.com (ORCID: 0000-0001-5963-5295)

1.25–13.79) and unclear lymphatic gate structure (OR=19.20, 95% CI: 1.98–186.36) were identified as independent risk factors of axillary lymph node metastasis in patients with lateral quadrant breast cancer. Furthermore, a nomogram model was developed to predict axillary lymph node metastasis in lateral quadrant breast cancer cases. The ROC curves showed that the area under the curve (AUC) for the training set was 0.74 (95% CI: 0.62–0.86) and the AUC for the validation set was 0.73 (95% CI: 0.62–0.84). Hosmer-Lemeshow test results indicated no significant deviation from goodness-of-fit for both the training set and validation set with *P*-values of 0.570 and 0.552, respectively. **Conclusion:** Ultrasound plays a valuable role in the assessment of axillary lymph node metastasis in patients with lateral quadrant breast cancer. The nomogram prediction model based on logistic regression demonstrates good safety, reliability, and practicality for clinical use.

[Key words] ultrasound; lateral quadrant breast cancer; axillary lymph node metastasis; nomogram model; logistic regression

[J Nanjing Med Univ, 2025, 45(01): 13-21]

乳腺癌是女性常见的恶性肿瘤,严重威胁女性健康<sup>[1]</sup>。乳腺癌常见于外侧象限,而该区域肿瘤易发生腋窝淋巴结转移<sup>[2-3]</sup>。由于乳房淋巴管的外部引流通向腋下,因此外侧象限肿瘤容易通过这一途径到达腋下,导致腋窝淋巴结转移<sup>[4]</sup>。腋窝淋巴结作为主要的转移途径,是影响乳腺癌预后的重要危险因素<sup>[5-6]</sup>。根据美国国立综合癌症网络指南,明确腋窝淋巴结是否转移对乳腺癌准确分期至关重要,同时与临床精准治疗方案的制定密切相关<sup>[7]</sup>。

目前,超声引导下的淋巴结穿刺活检和淋巴结手术活检被认为是获得病理的最有效途径<sup>[8]</sup>。虽然穿刺活检获取淋巴结病理的方法在临床实践中得到广泛应用,但可能引起一定的并发症,如出血、淋巴漏、感染、血肿等,影响临床治疗<sup>[9]</sup>。临床常用无创检查包括钼靶、电子计算机断层扫描(computed tomography, CT)、B型超声。钼靶能够清晰地显示乳腺结构及病变,但不能对腋窝淋巴结进行精准评价<sup>[10]</sup>。CT具有较高的空间和密度分辨率,但对于较小转移淋巴结的识别存在一定局限性,同时伴有辐射风险<sup>[11]</sup>。超声在乳腺癌原发肿瘤及局部淋巴结检测中以其方便、快速、无辐射等优点成为应用最广泛的一种评估方法,在临床实践中得到了广泛推广<sup>[12]</sup>。然而,基于超声的乳腺癌患者腋窝淋巴结转移的列线图预测模型尚未建立。因此,本研究回顾性分析了乳腺癌肿瘤和腋窝淋巴结的超声特征,并结合淋巴结的病理结果,构建并验证了一个新的列线图预测模型,旨在为临床评估腋窝淋巴结转移提供一个简单高效的诊断工具。

## 1 对象和方法

### 1.1 对象

本回顾性队列研究纳入了2020年1月—2023

年12月在无锡市锡山人民医院收治的外侧象限乳腺癌患者共127例,伴腋窝淋巴结转移患者54例为阳性组,不伴腋窝淋巴结转移患者73例为阴性组。

纳入标准:①术前行详细乳腺肿瘤及腋窝淋巴结B超检查的外侧象限乳腺癌患者,并留存规范超声图像者;②行乳腺癌根治性手术及前哨淋巴结活检或术前腋窝淋巴结活检,并有明确腋窝淋巴结病理诊断者。排除标准:①术前未行腋窝淋巴结超声检查;②乳腺癌患者的非手术治疗;③复发性乳腺癌;④有乳腺癌放疗、化疗及内分泌治疗病史。本研究符合《赫尔辛基宣言》,经过无锡市锡山人民医院伦理委员会的批准(xs2024ky037)。

### 1.2 方法

所有患者术前均行乳腺肿瘤及腋窝淋巴结的超声检查。由经验丰富的乳腺超声医生完成。采用VolusonE10、LogiqE9(GE医疗系统有限公司,美国)及Epiq7(飞利浦超声股份有限公司,荷兰)彩色多普勒超声诊断仪。本研究所有图像分析均由2名有5年以上乳腺超声诊断经验的医生独立进行。当出现意见不合时,由高级职称医生统一意见。详细分析乳腺病变的超声图像特征,包括乳腺肿瘤位置、生长方式(垂直或水平)、肿瘤直径、回声(低或高)、内部回声(不均匀或均匀)、边缘(不光整或光整)、形态(不规则或规则)、针状边缘(否或是)、角边(否或是)、高回声晕(否或是)、后方回声衰减(否或是)、钙化(否或是)、血液供应(少/中等或丰富)。分析超声图像上区域淋巴结的特征,包括淋巴结形态(不规则或规则)、淋巴结生长方式(垂直或水平)、淋巴结内部回声(不均匀或均匀)、皮质厚度(增厚或正常)、淋巴门结构(不清晰或清晰)、淋巴结血液供应(少/中等或丰富)。

### 1.3 统计学方法

数据分析采用SPSS22.0和R4.0.3统计软件。连续数据使用Shapiro正态性检验,正态分布数据以均数±标准差( $\bar{x} \pm s$ )表示,采用Student's *t*检验。非正态分布数据以中位数(四分位数)[ $M(P_{25}, P_{75})$ ]表示,采用Wilcoxon检验。分类数据以频率和构成比表示,采用卡方检验或Fisher精确检验。应用lrm函数进行二元Logistic回归分析,然后采用stepAIC函数的后退法进行自变的筛选,最后使用二元Logistic回归分析构建列线图。使用pROC函数绘制受试者工作特征曲线(receiver operating characteristic curve, ROC),计算曲线下面积(area under the curve, AUC)。 $P < 0.05$ 为差异有统计学意义。

## 2 结果

### 2.1 阳性组和阴性组乳腺肿瘤及腋窝淋巴结超声特征比较

127例外侧象限乳腺癌患者根据排除和纳入标准被纳入本研究,阳性组54例,阴性组73例。总结并分析乳腺癌患者乳腺肿瘤和腋窝淋巴结的超声特征。与阴性组相比,阳性组肿瘤低回声比例低,针状边缘比例高( $P < 0.05$ ,表1)。此外,阳性组的淋巴结形态不规则、内部回声不均匀、皮质增厚、淋巴门结构不清晰以及淋巴结血流丰富比例更高( $P < 0.05$ ,表2)。

### 2.2 训练集和验证集的特征资料比较

通过R语言将数据集随机分为训练集和验证集。63例患者纳入训练集,64例患者纳入验证集。通过特征资料的比较,两组乳腺肿瘤超声特征仅在后方回声方面存在差异( $P=0.017$ ,表3),腋窝淋巴结超声特征无明显差异(表4),结果提示两组分配合理。

### 2.3 腋窝淋巴结转移相关超声特征的筛选

为了进一步探讨腋窝淋巴结转移相关肿瘤及腋窝淋巴结的超声特征,使用单因素Logistic回归分析发现肿瘤针状边缘(OR=3.26, 95%CI: 1.13~9.43,  $P=0.029$ )、淋巴结皮质增厚(OR=7.78, 95%CI: 1.87~32.34,  $P=0.005$ )和淋巴门结构不清晰(OR=14.39, 95%CI: 1.64~125.98,  $P=0.016$ )是腋窝淋巴结转移的危险因素。进一步多因素分析结果显示,肿瘤针状边缘(OR=4.16, 95%CI: 1.25~13.79,  $P=0.020$ ,图1A)和淋巴门结构不清晰(OR=19.20, 95%CI: 1.98~186.36,  $P=0.011$ ,图1B)是腋窝淋巴结转移的独立危险因素(表5)。

### 2.4 腋窝淋巴结转移列线图预测模型的构建及验证

基于多因素回归分析结果,纳入乳腺肿瘤针状边缘、腋窝淋巴结淋巴门结构不清晰,建立列线图预测模型(图2A)。ROC曲线显示,训练集的AUC为0.74(0.62~0.86,图2B),验证集的AUC为0.73(0.62~0.84,图2C),具有良好的诊断性能。校准图显示了在训练集和验证集中的预测图和实际列线图之间的一致性(图2D、E)。同时,训练集的Hosmer-Lemeshow检验 $P=0.570$ ,验证集的Hosmer-Lemeshow检验 $P=0.552$ , $P$ 均 $>0.05$ ,说明列线图的预测值与实际列线图的预测值无明显差异。最后,绘制临床决策曲线,结果显示该模型在训练集和验证集上都远离极端曲线,说明所构建的列线图预测模型是安全、可靠、实用的(图2F、G)。

## 3 讨论

在上世纪末,尽管乳腺癌的发病率逐年增加,但其病死率下降了约43%<sup>[13]</sup>。乳腺癌的早期筛查、诊断和治疗在其中起着重要作用。乳腺癌好发于外侧象限,而同侧腋窝淋巴结是外侧乳腺癌患者最早、最常见的转移途径<sup>[14]</sup>。研究表明,腋窝淋巴结转移是乳腺癌复发和影响长期生存的危险因素<sup>[5-6]</sup>。而且,术前准确评估腋窝淋巴结的状态对于分期、术式选择、制定治疗方案都有非常重要的意义<sup>[15-16]</sup>。超声成像具有较高的空间分辨率,与CT和/或磁共振相比更易于检测异常的淋巴结,是观察异常淋巴结特征的首选方法<sup>[17-18]</sup>。而且超声由于其管理方便、设备便携性高、成本低等优点,有利于临床推广<sup>[12]</sup>。通过超声检测到的特征来预测淋巴结转移具有显著优势。

本研究回顾性分析了外侧象限乳腺癌患者的肿瘤和腋窝淋巴结的超声影像学特征,发现针状边缘、淋巴门结构不清晰是外侧象限乳腺癌伴腋窝淋巴结转移的独立危险因素。针状边缘又称毛刺征,超声表现为从肿块向边缘放射状分布的线状突出物,超声特征明显,一般较易识别。针状边缘是由于肿瘤呈浸润性生长,导致周围结缔组织反应性增生形成<sup>[19]</sup>。针状边缘可反映肿瘤浸润性生长的特性,而且针状边缘越明显,说明肿瘤侵袭性越强,发生转移的风险越大<sup>[20]</sup>。本研究提示腋窝淋巴结转移组肿瘤具有更高比例的针状边缘特征。孙芳等<sup>[21]</sup>研究也证实肿瘤针状边缘是乳腺癌淋巴结转移的危险因素。淋巴门是淋巴结的正常结构,常位于淋巴结的中央。当恶性肿瘤细胞侵入淋巴结时可破坏淋

表1 腋窝淋巴结转移阳性组和阴性组乳腺肿瘤超声特征比较

Table 1 Comparison of ultrasound characteristics of breast tumors between the positive and negative axillary lymph node metastasis groups

Characteristic	Negative group(n=73)	Positive group(n=54)	P
Age(years, $\bar{x} \pm s$ )	62.53 ± 12.08	58.67 ± 12.32	0.079
Growth pattern[n(%)]			
Vertical	6(8.2)	4(7.4)	0.869
Horizontal	67(91.8)	50(92.6)	
Tumor diameter[mm, M(P <sub>25</sub> , P <sub>75</sub> )]	20.0(15.0, 27.0)	23.5(18.0, 30.0)	0.103
Echo[n(%)]			0.013
Low	73(100.00)	48(88.89)	
High	0(0)	6(11.11)	
Internal echo[n(%)]			0.450
Homogeneity	22(30.14)	13(24.07)	
Heterogeneity	51(69.86)	41(75.93)	
Margin[n(%)]			0.910
Smooth	6(8.22)	5(9.26)	
Unsmooth	67(91.78)	49(90.74)	
Form[n(%)]			0.968
Regular	11(15.07)	8(14.81)	
Irregular	62(84.93)	46(85.19)	
Spiculated margins[n(%)]			0.007
No	42(57.53)	18(33.33)	
Yes	31(42.47)	36(66.67)	
Corner edge[n(%)]			0.516
No	56(76.71)	44(81.48)	
Yes	17(23.29)	10(18.52)	
Hyperechoic halo[n(%)]			0.417
No	70(95.89)	49(90.74)	
Yes	3(4.11)	5(9.26)	
Rear echo attenuation[n(%)]			0.350
No	65(89.04)	45(83.33)	
Yes	8(10.96)	9(16.67)	
Calcification[n(%)]			0.625
No	37(50.68)	25(46.30)	
Yes	36(49.32)	29(53.70)	
Blood suppl[n(%)]			0.643
Less/Moderate	63(86.30)	45(83.33)	
Abundant	10(13.70)	9(16.67)	

表2 腋窝淋巴结转移阳性组和阴性组腋窝淋巴结超声特征比较

Table 2 Comparison of ultrasound characteristics between the axillary lymph node metastasis-positive and negative groups in the axilla [n(%)]

Ultrasound characteristic	Negative group(n=73)	Positive group(n=54)	P	Ultrasound characteristic	Negative group(n=73)	Positive group(n=54)	P
Lymph node morphology			0.030	Cortical thickness			<0.001
Regular	71(97.26)	46(85.19)		Normal	67(91.78)	33(61.11)	
Irregular	2(2.74)	8(14.81)		Thicken	6(8.22)	21(38.89)	
Lymph node growth pattern			0.425	Lymphatic hilum structure			<0.001
Vertical	0(0)	1(1.85)		Clear	70(95.89)	38(70.37)	
Horizontal	73(100.00)	53(98.15)		Unclear	3(4.11)	16(29.63)	
Echoes inside lymph nodes			0.030	Blood suppl			0.030
Homogeneity	71(97.26)	46(85.19)		Less/Moderate	71(97.26)	46(85.19)	
Inhomogeneity	2(2.74)	8(14.81)		Abundant	2(2.74)	8(14.81)	

表3 训练集和验证集乳腺肿瘤超声特征比较

Table 3 Comparison of breast tumor B-ultrasound characteristics between the training and validation datasets

Characteristic	Training set(n=63)	Validation set(n=64)	P
Age( $\bar{x} \pm s$ )	60.97 ± 10.88	60.81 ± 13.62	0.943
Growth pattern[n(%)]			0.722
Vertical	6(9.52)	4(6.25)	
Horizontal	57(90.48)	60(93.75)	
Tumor diameter[mm, M(P <sub>25</sub> , P <sub>75</sub> )]	22.0(15.0, 28.5)	22.0(16.0, 30.0)	0.935
Echo[n(%)]			0.217
Low	62(98.41)	59(92.19)	
High	1(1.59)	5(7.81)	
Internal echo[n(%)]			0.515
Homogeneity	44(69.84)	48(75)	
Heterogeneity	19(30.16)	16(25)	
Margin[n(%)]			0.773
Smooth	5(7.94)	6(9.38)	
Unsmooth	58(92.06)	58(90.62)	
Form[n(%)]			0.478
Regular	8(12.70)	11(17.19)	
Irregular	55(87.30)	53(82.81)	
Spiculated margins[n(%)]			0.660
No	31(49.21)	29(45.31)	
Yes	32(50.79)	35(54.69)	
Corner edge[n(%)]			0.793
No	49(77.78)	51(79.69)	
Yes	14(22.22)	13(20.31)	
Hyperechoic halo[n(%)]			0.263
No	57(90.48)	62(96.88)	
Yes	6(9.52)	2(3.12)	
Rear echo attenuation[n(%)]			0.017
No	50(79.37)	60(93.75)	
Yes	13(20.63)	4(6.25)	
Calcification[n(%)]			0.533
No	29(46.03)	33(51.56)	
Yes	34(53.97)	31(48.44)	
Blood suppl[n(%)]			0.832
Less/Moderate	54(85.71)	54(84.38)	
Abundant	9(14.29)	10(15.62)	

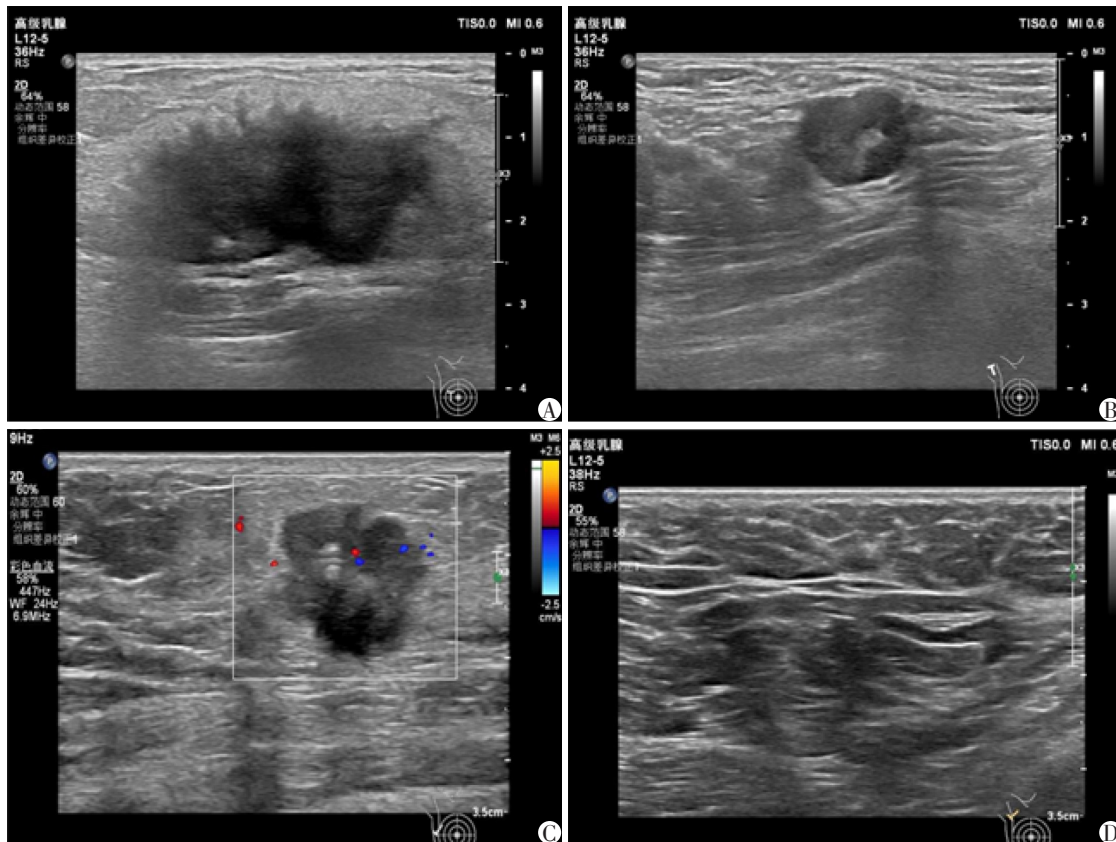
表4 训练集和验证集腋窝淋巴结超声特征比较

Table 4 Comparison of ultrasound features of axillary lymph nodes between the training and validation datasets [n(%)]

Ultrasound characteristic	Training set(n=63)	Validation set(n=64)	P	Ultrasound characteristic	Training set(n=63)	Validation set(n=64)	P
Lymphatic metastasis			0.521	Cortical thickness			0.864
No	38(60.32)	35(54.69)		Normal	50(79.37)	50(78.12)	
Yes	25(39.68)	29(45.31)		Thicken	13(20.63)	14(21.88)	
Lymph node morphology			0.761	Lymphatic hilum structure			0.478
Regular	58(92.06)	59(92.19)		Clear	55(87.30)	53(82.81)	
Irregular	5(7.94)	5(7.81)		Unclear	8(12.70)	11(17.19)	
Lymph node growth pattern			0.496	Blood suppl			0.761
Vertical	1(1.59)	0(0)		Less/Moderate	59(93.65)	58(90.62)	
Horizontal	62(98.41)	64(100.0)		Abundant	4(6.35)	6(9.38)	
Echoes inside lymph nodes			0.336				
Homogeneity	60(95.24)	57(89.06)					
Inhomogeneity	3(4.76)	7(10.94)					

表5 训练集单因素和多因素Logistics回归分析  
Table 5 Univariate and multivariate logistic regression analysis of the training set

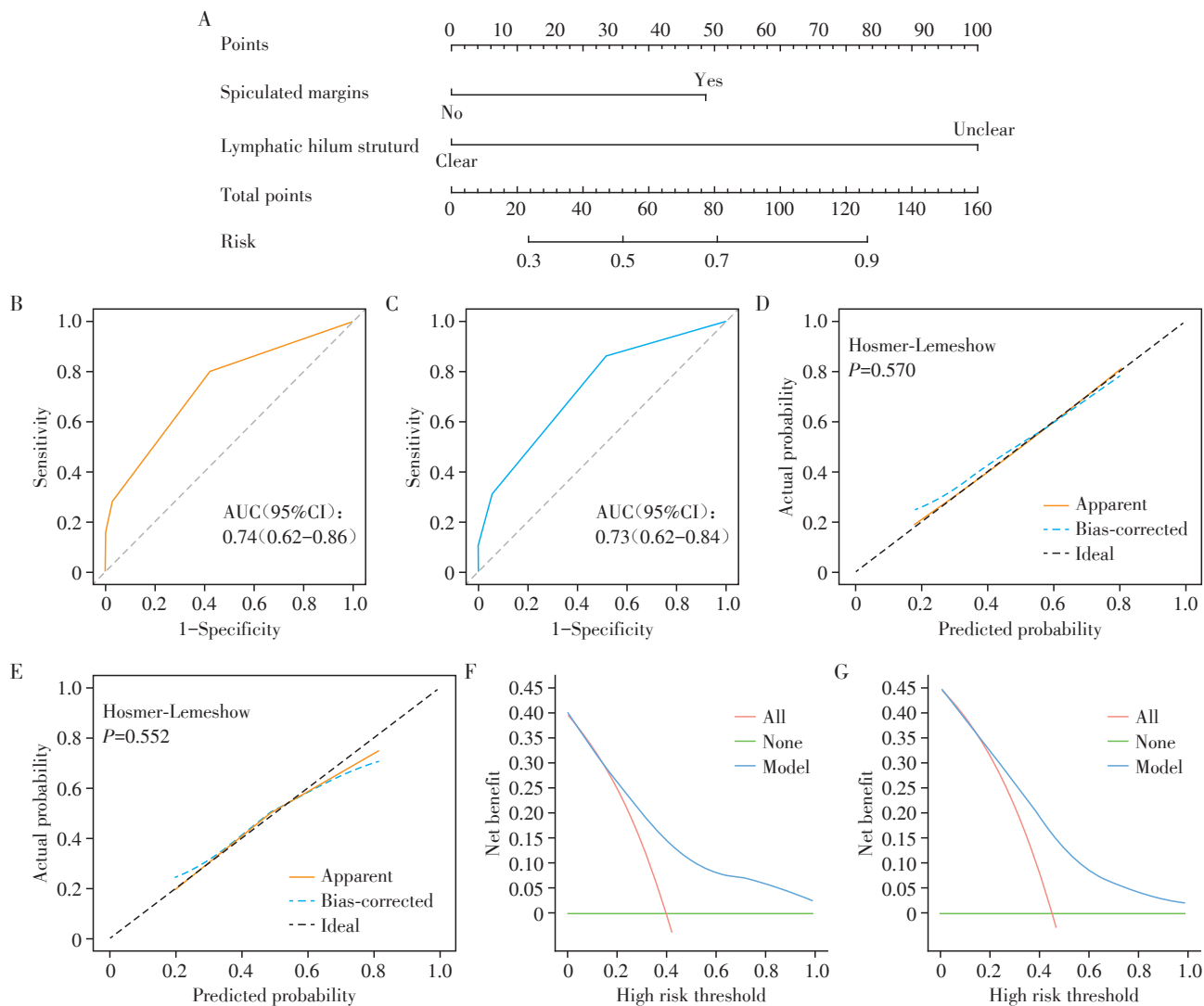
Variable	Univariate analysis		Multivariate analysis	
	OR(95%CI)	P	OR(95%CI)	P
Growth pattern	0.74(0.12-4.37)	0.739		
Tumor diameter	1.01(0.96-1.06)	0.838		
Echo	9 116 537.03(0-Inf)	0.991		
Internal echo	0.87(0.29-2.59)	0.796		
Margin	2.82(0.30-26.86)	0.366		
Form	2.16(0.40-11.66)	0.372		
Spiculated margins	3.26(1.13-9.43)	0.029	4.16(1.25-13.79)	0.020
Corner edge	0.81(0.23-2.76)	0.731		
Hyperechoic halo	1.59(0.29-8.59)	0.590		
Rear echo attenuation	2.07(0.60-7.12)	0.247		
Calcification	1.98(0.70-5.56)	0.198		
Tumor blood suppl	1.26(0.30-5.22)	0.753		
Lymph node morphology	7.05(0.74-67.25)	0.090		
Lymph node growth pattern	9 116 537.03(0-Inf)	0.991		
Echoes inside lymph nodes	3.22(0.28-37.52)	0.351		
Cortical thickness	7.78(1.87-32.34)	0.005	2.52(0.35-18.11)	0.359
Lymphatic hilum structure	14.39(1.64-125.98)	0.016	19.20(1.98-186.36)	0.011
Lymph node blood suppl	5.05(0.49-51.54)	0.172		



A: Ultrasound image of breast tumor in a patient with axillary lymph node metastasis, showing spiculated margins. B: Ultrasound feature of axillary lymph nodes in a patient with axillary lymph node metastasis, displaying an unclear cortical structure. C: Ultrasound image of breast tumor in a patient without axillary lymph node metastasis. D: Ultrasound image of axillary lymph nodes in a patient without axillary lymph node metastasis.

图1 外侧象限乳腺癌患者腋窝淋巴结转移与未转移患者的乳腺肿瘤及腋窝淋巴结超声图像

Figure 1 Ultrasound images of breast tumors and axillary lymph nodes in patients with lateral quadrant breast cancer, showing metastasis and non-metastasis in the axillary lymph nodes



A: Nomogram model based on training set. B: ROC curve for the nomogram predicting of training set. C: ROC curve for the nomogram predicting of validation set. D: Calibration curve for the nomogram predicting of training set. E: Calibration curve for the nomogram predicting of validation set. F: Decision curve analysis for the nomogram predicting of training set. G: Decision curve analysis for the nomogram predicting of validation set.

图2 预测外侧象限乳腺癌患者腋窝淋巴结转移的列线图模型

Figure 2 Nomogram models for predicting axillary lymph node metastasis in patients with lateral quadrant breast cancer

巴结结构, 早期表现为淋巴结皮质不均匀增厚, 晚期表现为淋巴门结构消失<sup>[22]</sup>。本研究与既往研究一致, 淋巴门结构不清晰是诊断腋窝淋巴结转移的重要特征<sup>[23]</sup>。由此可见, 本研究筛选得到的肿瘤针状边缘和淋巴门结构不清晰是腋窝淋巴结转移的危险因素, 这一观点与既往研究保持一致。

事实上, 基于超声图像特征构建的淋巴结转移预测模型已被报道, 这在术前评估中起着重要作用<sup>[24]</sup>。Zhang等<sup>[25]</sup>收集755例早期乳腺癌患者的超声图像, 采用最大相关和最小冗余算法、最小绝对值收敛和选择算子方法构建的预测模型具有良好的预测效果。另一项基于176例早期乳腺癌患者的超声图像构建的列线图, 其训练集和测试集的AUC

分达到了0.900和0.821<sup>[26]</sup>。这些研究均表明超声特征构建的预测模型具有较好的诊断效能。多数研究关注早期乳腺癌淋巴结转移的诊断, 本研究主要针对易发生腋窝淋巴结转移的不同分期的外侧象限肿瘤, 能够给不同分期的患者提供指导; 本研究构建预测模型所选择的关键因素与其他研究不同, 是基于2个显著相关的超声特征构建, 更加简单方便; 而且校准图和临床决策曲线结果均显示良好。因此, 本研究构建的新的列线图预测模型对于预测外侧象限乳腺癌患者的腋窝淋巴结转移具有重要临床意义。此外, 这种预测的列线图模型可能有助于制定诊断和治疗策略, 并有利于未来更多的患者。

本研究基于超声图像分析, 筛选了外侧象限乳

腺癌腋窝淋巴结转移的危险因素,同时构建了一个新的列线图预测模型,并具有良好的诊断性能。然而也有一定的局限性。本研究的数据仅来源于单一中心,患者的异质性也仅限于周边地区,与中国乃至世界各地的全体人口相比,疾病分布仍存在显著差异。此外,种族异质性未被纳入本研究。因此,多中心合作可能有助于弥补这些缺陷。同时,该预测模型仍缺乏临床实践和验证,未来需要有更严格的后续研究以期获得更好的反馈。

综上,随着乳腺癌发病率的逐年上升,采用有效方法进行早期筛查和诊断是提高治疗效果的重要手段。超声在检测乳腺癌患者的区域淋巴结方面具有方便、快速、直观、可重复性好等优点。本研究基于 Logistic 回归方法回顾性分析超声图像,构建了列线图预测模型,具有良好的诊断效能,可以进一步推广实施,有助于更好地评估外侧象限乳腺癌患者的腋窝淋巴结转移。

#### 利益冲突声明:

所有作者均声明没有利益冲突。

#### Conflict of Interests:

The authors declare no competing interests.

#### 作者贡献声明:

陈超波、朱美娣:研究设计及论文撰写。许紫鹏:统计学方法设计。朱美娣、华玲玲:数据的收集与分析。秦菲、房玲:文章审阅。

#### Author's Contributions:

All authors have read and approved the final manuscript. CHEN Chaobo and ZHU Meidi: designed the research and drafted the paper. XU Zipeng: designed the mathematical methods. ZHU Meidi and HUA Lingling: collected and analyzed the data. QIN Fei and FANG Ling: reviewed this paper.

#### [参考文献]

- [1] SIEGEL R L, GIAQUINTO A N, JEMAL A. Cancer statistics, 2024[J]. CA Cancer J Clin, 2024, 74(1): 12-49
- [2] CHEN K, LIU J, LI S, et al. Development of nomograms to predict axillary lymph node status in breast cancer patients[J]. BMC Cancer, 2017, 17(1): 561
- [3] MANJER J, BALLDIN G, GARNE J P. Tumour location and axillary lymph node involvement in breast cancer: a series of 3472 cases from Sweden[J]. Eur J Surg Oncol, 2004, 30(6): 610-617
- [4] ESTOURGIE S H, NIEWEG O E, OLMOS R A, et al. Lymphatic drainage patterns from the breast [J]. Ann Surg, 2004, 239(2): 232-237
- [5] KUEMMEL S, HEIL J, BRUZAS S, et al. Safety of targeted axillary dissection after neoadjuvant therapy in patients with node-positive breast cancer[J]. JAMA Surg, 2023, 158(8): 807-815
- [6] ZHU T, HUANG Y H, LI W, et al. Multifactor artificial intelligence model assists axillary lymph node surgery in breast cancer after neoadjuvant chemotherapy: multi-center retrospective cohort study[J]. Int J Surg, 2023, 109(11): 3383-3394
- [7] GRADISHAR W J, MORAN M S, ABRAHAM J, et al. NCCN guidelines (R) insights: breast cancer, version 4.2023[J]. J Natl Compr Canc Netw, 2023, 21(6): 594-608
- [8] LI C, ZHANG P, LV J, et al. Axillary management in patients with clinical node-negative early breast cancer and positive sentinel lymph node: a systematic review and meta-analysis[J]. Front Oncol, 2023, 13: 1320867
- [9] XIE S, JU S, ZHANG X, et al. A retrospective comparative study on the diagnostic efficacy and the complications: between Cassi II rotational core biopsy and core needle biopsy[J]. Front Oncol, 2023, 13: 1067246
- [10] 罗勇, 吴舟洋, 周菲菲, 等. 乳腺钼靶联合动态对比增强MRI检查在乳腺癌诊断及临床T分期中的价值[J]. 实用放射学杂志, 2022, 38(12): 1967-1970
- [10] LUO Y, WU Z Y, ZHOU F F, et al. The value of mammography combined with dynamic contrast-enhanced MRI indagnosis and clinical T-staging of breastcancer [J]. Journal of Practical Radiology, 2022, 38(12): 1967-1970
- [11] 杨亦, 姚钰, 刘家伟, 等. 多种影像学手段评估乳腺癌患者腋窝淋巴结状态的对比研究[J]. 南京医科大学学报(自然科学版), 2019, 39(5): 721-726
- [11] YANG Y, YAO Y, LIU J W, et al. A comparative analysis of various imaging techniques for assessing axillary lymph node status in breast cancer patients[J]. Journal of Nanjing Medical University (Nature Sciences), 2019, 39(5): 721-726
- [12] HAN P, YANG H, LIU M, et al. Lymph node predictive model with *in vitro* ultrasound features for breast cancer lymph node metastasis[J]. Ultrasound Med Biol, 2020, 46(6): 1395-1402
- [13] GIAQUINTO A N, SUNG H, MILLER K D, et al. Breast cancer statistics, 2022 [J]. CA Cancer J Clin, 2022, 72(6): 524-541
- [14] 师金, 梁迪, 李道娟, 等. 全球女性乳腺癌流行情况研究[J]. 中国肿瘤, 2017, 26(9): 683-690
- [14] SHI J, LIANG D, LI D J, et al. Epidemiological Status of Global Female Breast Cancer[J]. China Cancer, 2017, 26(9): 683-690
- [15] 刘心培, 查海玲, 平洁怡, 等. 超声监测定位腋窝淋巴结对乳腺癌患者新辅助治疗疗效的预测研究[J]. 南京医

- 科大学学报(自然科学版), 2024, 44(6): 845-852
- LIU X P, ZHA H, PING J Y, et al. Monitoring of clipped axillary lymph node by ultrasound to predict response of breast cancer to neoadjuvant systemic therapy [J]. Journal of Nanjing Medical University (Nature Sciences), 2024, 44(6): 845-852
- [16] ARJMANDI F, MOOTZ A, FARR D, et al. New horizons in imaging and surgical assessment of breast cancer lymph node metastasis [J]. Breast Cancer Res Treat, 2021, 187(2): 311-322
- [17] JUNN J C, SODERLUND K A, GLASTONBURY C M. Imaging of head and neck cancer with CT, MRI, and US[J]. Semin Nucl Med, 2021, 51(1): 3-12
- [18] EIDA S, FUKUDA M, KATAYAMA I, et al. Metastatic lymph node detection on ultrasound images using YO-LOv7 in patients with head and neck squamous cell carcinoma[J]. Cancers(Basel), 2024, 16(2): 274
- [19] MERCIDYL G T, ANDERS L, ERIK T, et al. Nonpalpable breast cancer: mammographic appearance as predictor of histologic type[J]. Radiology, 2002, 222(1): 165-170
- [20] 金家承, 陈鹏超. 超声影像学特征评估乳腺癌腋窝淋巴结转移的影响因素分析[J]. 浙江医学, 2023, 45(20): 2208-2211
- JIN J C, CHEN P C. An analysis of the factors influencing axillary lymph node metastasis in breast cancer based on ultrasound imaging characteristics [J]. Zhejiang Medical Journal, 2023, 45(20): 2208-2211
- [21] 孙芳, 杨智, 许永波, 等. 超声特征联合免疫组化构建列线图预测早期乳腺癌前哨淋巴结转移[J]. 中国超声医学杂志, 2022, 38(2): 146-150
- SUN F, YANG Z, XU Y B, et al. Ultrasound combined with immunohistochemistry to construct a nomogram to predict sentinel lymph node metastasis in early-stage breast cancer[J]. Chinese Journal of Ultrasound in Medicine, 2022, 38(2): 146-150
- [22] CUI Q L, YIN S S, FAN Z H, et al. Diagnostic value of contrast-enhanced ultrasonography and time-intensity curve in differential diagnosis of cervical metastatic and tuberculous lymph nodes[J]. J Ultrasound Med, 2018, 37(1): 83-92
- [23] LUO S, YAO G, HONG Z, et al. Qualitative classification of shear wave elastography for differential diagnosis between benign and metastatic axillary lymph nodes in breast cancer[J]. Front Oncol, 2019, 9: 533
- [24] CHANG L, ZHANG Y, ZHU J, et al. An integrated nomogram combining deep learning, clinical characteristics and ultrasound features for predicting central lymph node metastasis in papillary thyroid cancer: a multicenter study[J]. Front Endocrinol(Lausanne), 2023, 14: 964074
- [25] ZHANG W, WANG S, WANG Y, et al. Ultrasound-based radiomics nomogram for predicting axillary lymph node metastasis in early-stage breast cancer[J]. Radiol Med, 2024, 129(2): 211-221
- [26] ZHANG H, ZHAO T, ZHANG S, et al. Prediction of axillary lymph node metastatic load of breast cancer based on ultrasound deep learning radiomics nomogram[J]. Technol Cancer Res Treat, 2023, 22: 15330338231166218

[收稿日期] 2024-07-13

(本文编辑: 唐震)